



PLASMAS FOR TRANSITION DELAY

Marios Kotsonis¹, Pieter Boon², Leo Veldhuis³

ABSTRACT

This paper describes the experimental investigation of the properties of Dielectric Barrier Discharge (DBD) actuators aimed at transition delay techniques. A wide range of geometrical configurations are tested as well as several electrical operational conditions. For the majority of the measurements statistical data for the induced flow field are obtained and for a limited selection of actuators, high sample-rate time resolved measurements are also conducted. All measurements are made in still flow in order to eliminate free-stream effects on the induced velocities. Results show the formation of a thin near-wall jet which could be used as a flow control device.

Keywords: plasma actuators, experimental study, active wave cancellation, transition delay

INTRODUCTION

Delft University of Technology has recently launched the multidisciplinary project “CleanEra” with the goal of developing new technologies to meet the EU Vision 2020 requirements for the next generation environmentally friendly transport aircraft. Several key topics are being developed including aerodynamic drag reduction. The current work lies within the scope of drag reduction through boundary layer transition delay techniques. More specifically the chosen method is based on the direct wave cancellation of Tollmien-Schlichting (TS) modes with the use of plasma actuators as “counter-waves” introduction devices. This paper describes the experimental investigation of the performance of plasma actuators under various geometrical configurations and electrical operational conditions. The aim for this investigation is to identify the “key parameters” of the plasma actuator for the intended application of TS wave cancellation. To this goal an experimental parametric study is conducted to map the behavior of the plasma actuator under various parameters such as electrode width, dielectric thickness, applied voltage etc. Furthermore an investigation into the pulsed operation of the actuator is done to simulate the actual “counter-wave” introduction process and study the response of the flow under it.

In this paper, a brief introduction into the concept of wave cancellation and plasma actuators is given. Next an account of previous work on the subject is presented. An explanation of the experimental setup and of the experimental matrices is given in the next section. Last the results are presented, with discussion on the conclusions and future work.

¹ Corresponding author: PhD Researcher, Delft University of Technology, The Netherlands, e-mail: m.kotsonis@tudelft.nl

² MSc student, Delft University of Technology, The Netherlands

³ Associate Professor, Delft University of Technology, The Netherlands

Wave cancellation for transition delay

Transition from laminar to turbulent flow occurs in modern subsonic airliners at approximately 40% of the chord distance and it is primarily based on two mechanisms. These involve the development, amplification and final breakdown of two boundary-layer instability modes known as crossflow instabilities and Tollmien-Schlichting waves respectively. The dominance of each mechanism over the entire transition process is a function of the sweep angle. With increasing sweep angle, crossflow instabilities dominate over TS waves while for small sweep angles, TS is the dominant mode. The focus of this work is placed on TS waves, although an extension of the theory can be applied to crossflow as long as the linearity of the system is preserved.

Schlichting & Gersten (2000) report that turbulent flow is responsible for skin friction values of almost an order of magnitude larger than laminar flow. The large potential in skin friction drag reduction has led to considerable efforts in addressing the transition problem both with passive and active techniques. Passive or hybrid techniques such as Natural Laminar Flow (NLF) or Hybrid Laminar Flow Control (HLFC) have proven successful although, especially for HLFC, maintenance and reliability issues have kept them from full scale commercial applications. This has led to continuous research on alternative active flow control techniques which demonstrate equal performance as HLFC although with increased robustness and, eventually, a larger potential for a “real-world” application.

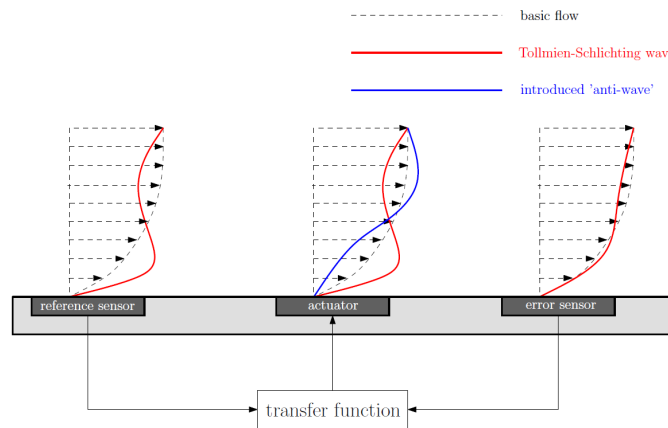


Figure 1. Concept of active TS wave cancellation

Apart from HLFC, other active flow control techniques have been successfully investigated. One particularly interesting method is the active cancellation of TS waves (Figure 1). This relies on the initial linearity of the growing TS waves and uses a superimposed artificially generated “counter-wave” to dampen the instability mode. In cruise conditions the TS modes develop in wavetrains within the boundary-layer that contain a spectrum of frequencies. In order to cancel them an integrated closed-loop feedback system has to be used employing sensors, actuators and processors. The sequence of actions in the feedback loop is based on sensing the incoming instability with a reference sensor. The signal is sent to a processor which uses a transfer function to define the frequency and phase of the wave and generate the “cancelling” signal. This activates the actuator which creates the “counter-wave” and introduces it in the laminar boundary-layer. An error sensor is used to monitor the resulting dampened wave and give a feedback signal back to the transfer function. The entire process is based on the initial linear amplification of the TS waves but the complete cancellation of the waves is not possible due to the unstable nature of

the boundary layer. Nevertheless, as long as the wavetrain is kept in this linear stage, the cancellation process can continue with the use of downstream placed actuators prolonging the transition area even further.

Plasma actuators

The insight that has been gained through HLFC research indicates that active flow control techniques have to be at least as robust as passive techniques in order to be applied on commercial aircraft. This translates directly to the need of more robust active flow control systems, namely sensors and actuators. As previously mentioned, the main concept of this work involves the direct cancellation of convective instabilities that grow within the laminar boundary layer, namely TS waves. To this end a new device is proposed for application, the Dielectric Barrier Discharge (DBD) actuator or plasma actuators.

Plasma actuators are a fairly new type of airflow control device, albeit with very attractive characteristics. There are two main types of actuators which have been extensively studied for flow control. These are the DBD actuator and the corona discharge actuator. The working principle is based on the ionization of air through high voltage (HV). For DBD the geometrical configuration consists of two thin electrodes separated by an also thin dielectric layer which acts as an insulator (Figure 2). The electrodes are placed flat on the wall of the aerodynamic surface (for example the wing). Normally the covered electrode, which lies below the dielectric, is kept at ground potential while the alternating HV is applied to the exposed to air upper electrode. A high electric field is then created with maximum intensity near the inner edges of the electrodes and ionizes the air. The ionized air consists of negative and positive ion as well as free electrons. These move under the influence of the electric field and through collisional processes transfer momentum to the neutral particles of air. Due to the asymmetric shape of the actuator and the presence of the dielectric which acts as a barrier for charged species, the transfer of momentum is not equal between the two cycles of the alternating voltage. This is macroscopically perceived as a directional body force vector acting on the free flow. In general the body force accelerates the flow in the direction from the exposed electrode towards the covered electrode.

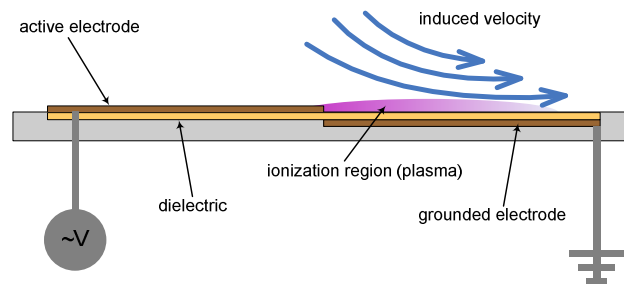


Figure 2. The DBD actuator and its operation

PREVIOUS WORK

Transition delay through cancellation of instability waves could be a promising field for low power actuators. Such technique was introduced by Thomas (1983) where vibrating ribbons were used to introduce and cancel single frequency TS waves. A numerical investigation of the same technique was carried out by Bower et al. (1987) with similar results. The waves were cancelled by simulated blowing or suction at the wall. These initial studies were concentrated on monochromatic waves mainly for validating the concept. This is only a very special case which is far from the actual flight conditions where a spectrum of frequencies randomly develop and amplify. The problem of naturally occurring TS waves

was recently attacked by Sturzebecher & Nitsche (2003) and Engert et al. (2007). Both experimental studies used vibrating membranes as actuators coupled to a closed-loop feedback system. Considerable delay of transition of up to 18% of chordwise distance compared to no actuation was achieved. Finally a very recent investigation using plasma actuators was carried by Grundmann and Tropea (2008). This study, which is comparable to the aspects of this work, dealt with single frequency waves and initial results were successful. One of the goals of the authors is to extend this concept to naturally occurring multi-frequency TS waves.

Plasma actuators have been studied extensively in recent years as flow control devices. In an early study Roth et al. (2000) used various flow diagnostics for different configurations of electrodes. They report a significant amount of thrust for asymmetrically placed spanwise actuators. Post and Corke (2004) showed successful separation control on airfoils at high angles of attack at subsonic speeds with the use of leading edge spanwise actuators. They show that the plasma operation accelerates the flow in the boundary layer and thus making it more resilient to separation. Jacob et al. (2004) and Huang et al. (2006) studied the effects of plasma actuators on boundary layer flow with considerable acceleration of the near-wall flow. This led to complete reattachment of flow over low pressure turbine blades. The general consensus of these separation control studies is that the plasma actuators, although capable of postponing separation at low Reynolds numbers, might not be as effective in higher velocity regimes. This has led to the investigation of other techniques which potentially will be also applicable in higher Reynolds numbers flows. Jukes et al. (2006) investigated the concept of induced spanwise flow oscillations through chordwise actuators. They proposed a physical mechanism which is analog to spanwise wall oscillations and registered considerable reduction in turbulent friction drag. Seraudie et al. (2006) studied the effects of DBD discharges on a laminar boundary layer. They report sufficient acceleration with simultaneous reduction in thickness. It is also evident that the effects diminish with increase in freestream velocities. Finally, a parametric study was conducted by Forte et al. (2007) in order to optimize the plasma actuator for airflow control.

EXPERIMENTAL SETUP

The DBD actuator

The actuators (Figure 3) consist of thin rectangular copper electrodes made out of self-adhesive copper tape. The thickness of the electrodes is 60 μm while the width varies between 5 mm and 25 mm. Their effective length (along which plasma is generated) is 200 mm. The electrodes are separated by several Kapton tape layers depending on the test case. The thickness of each layer is 2 mil (50.8 μm). The electrodes and dielectric are supported a 10 mm thick, 200x100 mm rectangular POM plate. The free ends of both electrodes are folded around the POM plate. The plate is then fixed on a rectangular POM base carrying two aluminum connectors which contact the electrodes. The connector of the upper electrode is connected to the HV output cable of a TREK® 20/20C HV amplifier (± 20 kV, ± 20 mA, 1000W) while the connector of the lower electrode is grounded. In this way the voltage is applied to the upper electrode while the lower remains grounded at all times. The design of the actuator was specifically chosen to be modular for the easy interchange of different configurations of electrodes. Also the POM base was designed to fit special slots in the Boundary Layer Tunnel (BLT) of the TU Delft for the experiments on transition which are currently under way.

The entire actuator operation is controlled remotely via a computer workstation. The driving signal is created via software and is sent to the amplifier via a Digital/Analog (D/A) converter. The amplifier has a fixed gain of 2000V/V and also provides direct readings of the output voltage and current through internal measurement probes. When the actuator is activated, plasma appears near the inner edge of the two

electrodes with decreased intensity towards the covered electrode. The ionization region appears to be uniform and constant along the length of the electrodes although it is known that it consists of multiple nanosecond discharges of high current flow.

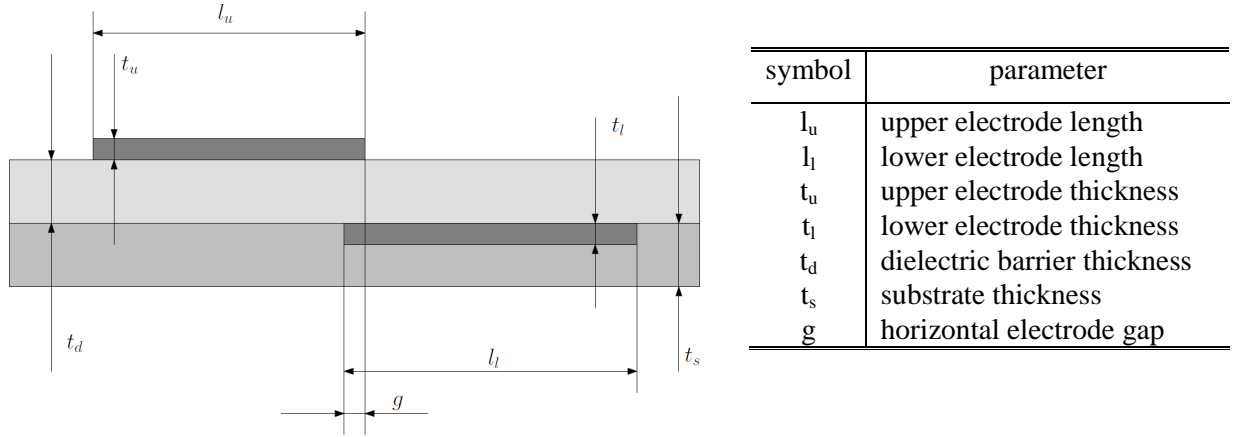


Figure 3. The main geometrical parameters of the DBD actuator

The test box

To reduce the effect of freestream velocity the tests are ran in still air. This approach has the advantage of increasing the accuracy of the measurements since the induced velocities are expected to be of the order of 1 m/s as well as giving more insight to the “pure” induced velocity field. On the other hand the major drawback of this approach is the lack of insight into the interaction process of the actuator and a given external flow. Although this is not a major issue for the parametric study of this work, experiments in the BLT are planned to this goal. For ensuring an environment of still air a box is constructed from clear Plexiglas. The box has the shape of a cube with a 500 mm long side. The base of the box has a, identical to the BLT, rectangular slot were the actuator fits in. In this way the actuator face is flushed with the base of the box thus minimizing any effects of roughness on the induced velocities. The box is equipped with ventilation due to the large amounts of ozone produced from the ionization process.

For the flow diagnostics Hot Wire Anemometry (HWA) is used. HWA has been found best suited for a parametric study as it combines sufficient accuracy with relative ease of use. For this study a Constant Temperature Anemometer (CTA) (TSI Inc. Model IFA300) is used with two single wire sensors. Based on an initial two-dimensionality study the flow has been identified as uniform and constant along the length of the electrodes. Based on this, any velocity component in the spanwise direction is considered negligible and the probes are placed in order to measure vertical velocity, v and total velocity, U . The horizontal velocity component, u , is derived from U and v .

Experimental matrices

Since this study is aiming at mapping the plasma actuator’s behavior as a wave-cancelling device, the goals of a parametric and optimization study are not so trivial. Unlike separation control techniques, the maximization of the induced velocity is not necessarily the main objective here. Instead, the induced velocity, its spatial extent and more importantly the temporal response of the flow have to be taken into account. The relatively simple construction of the DBD actuator enables a large number of geometric and material configurations that can be developed and tested. The same principle applies for the electrical

operating conditions. These increase the Degrees of Freedom (DoF) in a parametric study dramatically, to a point that a careful selection of control parameters has to be made in order to remain within reasonable limits of experimental time and resources consumption. The experiments are divided in three main groups.

Experiment group #1: geometrical properties

In experiment group #1 a parametric study is conducted on several geometrical variations. Statistical data (i.e averaged velocities) are obtained for a spatial mesh of points covering most of the downstream area of the actuator as well as a small part of the upstream area. Due to the nature of the ionization region, a small area cannot be approached by the hot-wires due to short-circuiting hazard. The mesh (Figure 4) consists of 89 non-uniformly positioned nodes for better resolution of the flow-field near the wall as well as near the actuator itself. The coordinate system presented here will be used throughout this paper. The origin is located 8 mm upstream from the inner edge of the upper electrode.

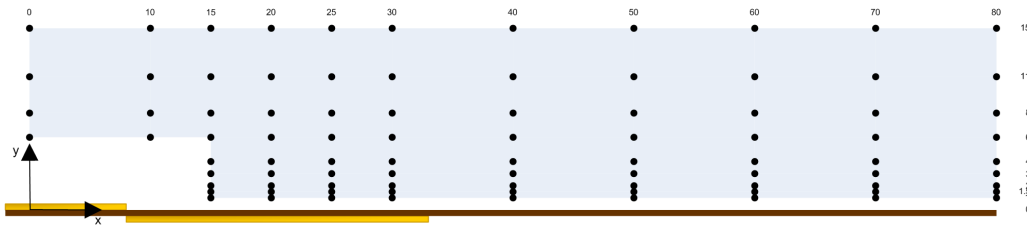


Figure 4. Measurement mesh for the experiment groups #1 and #2 (coordinates in mm)

Table 1. Parameters for experiment group #1

| Experiment group #1: geometrical properties (all lengths in mm) | | | | |
|---|-----------------------|--|--------------------|-----------------------|
| experiment # (control par.) | 1.1 (l _u) | 1.2 (l _l) | 1.3 (g) | 1.4 (t _d) |
| parameter | | | | |
| upper electrode length (l _u) | 5,10,15,20 | 10 | 10 | 10 |
| lower electrode length (l _l) | 25 | 5,10,15,20,25 | 25 | 25 |
| horizontal electrode gap (g) | 0 | 0 | -5,-2.5,0,1 | 0 |
| dielectric barrier thickness (t _d) | 0.058 | 0.058 | 0.116 | 0.058,0.116,0.174 |
| electrode thickness (t _u ,t _l) | | | 0.06 | |
| electrode material | | | copper | |
| dielectric material | | Kapton polyimide (relative permittivity 3.5) | | |
| applied voltage (V) | | | 8 kV _{pp} | |
| applied voltage frequency (F) | | | 2 kHz | |
| duty cycle (D) | | | 100% | |
| voltage waveform | | | sine | |

- Experiment group #2: electrical properties**

Experiment group #2 involves the investigation of the electrical operational values. These include voltage, frequency, pulsed frequency and duty cycle. The three best performing actuators, in terms of maximum induced velocity and spatial extent of the velocity field, of experiment group #1 are selected

for investigation of voltage and frequency. The best performing actuator from these three is selected for investigation of the waveform and pulsed operation. Additional high sample rate measurements of the voltage and current are done for waveform investigation. For the discharge current the amplifier's internal probe is not responsive enough to capture the micro-discharges. To this, the voltage across a resistance between the grounded electrode and the ground is read and converted to current.

Table 2. Parameters for experiment group #2

| Experiment group #2: electrical properties (all lengths in mm) | | | | | | | | | | |
|--|---|---------|----------------|----------------|-------------------|--|---------------|---|---|---|
| experiment # (control par.) | 2.1 (V_{app}) | 2.2 (F) | 2.3 (D) | 2.4 (f_p) | 2.5 (waveform) | | | | | |
| parameter | <ul style="list-style-type: none"> experiments 2.1 and 2.2 were done for three actuators: $[l_u=5, l_l=10], [l_u=10, l_l=10], [l_u=5, l_l=15]$ experiments 2.3, 2.4 and 2.5 were done for one actuator: $[l_u=5, l_l=15]$ | | | | | | | | | |
| upper electrode length (l_u) | | | | | | | | | | |
| lower electrode length (l_l) | | | | | | | | | | |
| horizontal electrode gap (g) | | | | | | 0 | | | | |
| dielectric barrier thickness (t_d) | | | | | | 0.116 | | | | |
| electrode thickness (t_u, t_l) | | | | | | 0.06 | | | | |
| electrode material | | | | | | copper | | | | |
| dielectric material | | | | | | Kapton polyimide (relative permittivity 3.5) | | | | |
| applied voltage (V_{app}) (kV _{pp}) | | | | | | 6,8,10,12 | 8 | 8 | 8 | 8 |
| applied voltage frequency (F) (kHz) | | | | | | 2 | 1,1.5,2,2.5,3 | 2 | 2 | 2 |
| duty cycle (D) (%) | 100 | 100 | 12.5,25,50,100 | 25 | 100 | | | | | |
| pulsed frequency (f_p) (Hz) | 0 | 0 | 100 | 50,100,150,200 | 0 | | | | | |
| voltage waveform | sine | sine | sine | sine | w1,w2,...w5 | | | | | |

- experiment group #3: time resolved pulsed operation

Due to the high importance of the pulsed operation in the conceptual process of active wave cancellation, a closer look is taken at. High sample rate (100000 samples/sec) measurements are taken for one actuator. A sub-matrix (Table 3.) of various combinations of duty cycles and pulsed frequencies is constructed and data are acquired for two downstream positions ($x = 7$ mm & $x = 15$ mm). Nevertheless, a considerable amount of points in the vertical to the wall direction (y direction) is taken for each downstream position. The HV amplifier voltage output monitor is also used for the simultaneous reading of the voltage supply. The actuator used is identical to the third actuator ($[l_u=5, l_l=15]$) of experiment 2.1 along with the same applied voltage (8 kV_{pp}) and frequency (2 kHz).

Table 3. Pulsed frequencies and duty cycles for experiment group #3

| Experiment group #3: time resolved pulsed operation | | | | | |
|---|---------------|---------------|---------------|---------------|---------------|
| pulsed frequency (f_p) (Hz) | 20 | 50 | 100 | 150 | 200 |
| duty cycle (D) (%) | 5,10,15,20,50 | 5,10,15,20,50 | 5,10,15,20,50 | 5,10,15,20,50 | 5,10,15,20,50 |

RESULTS

Experiment group #1: geometrical properties

For experiment group #1 parameters are shown in Table 1. The HWA measurements are done with a sample rate of 10000 Hz. The sample time is 1 sec. The data acquisition sample rate and time remain constant for experiment group #1 and #2. Typical measured flowfields for two different lengths of upper electrode are shown in (Figure 5). The induced flow appears in the form of a thin near-wall jet in the direction of the lower electrode. Also evident is a downwash flow behind the actuator although due to limitations in the use of HWA this could not be sufficiently resolved. Future PIV measurements are planned to this goal. The general behavior of the flow agrees with previously reported experimental and numerical studies reviewed by Corke et al.(2007) and Jayaraman & Shyy (2008) respectively.

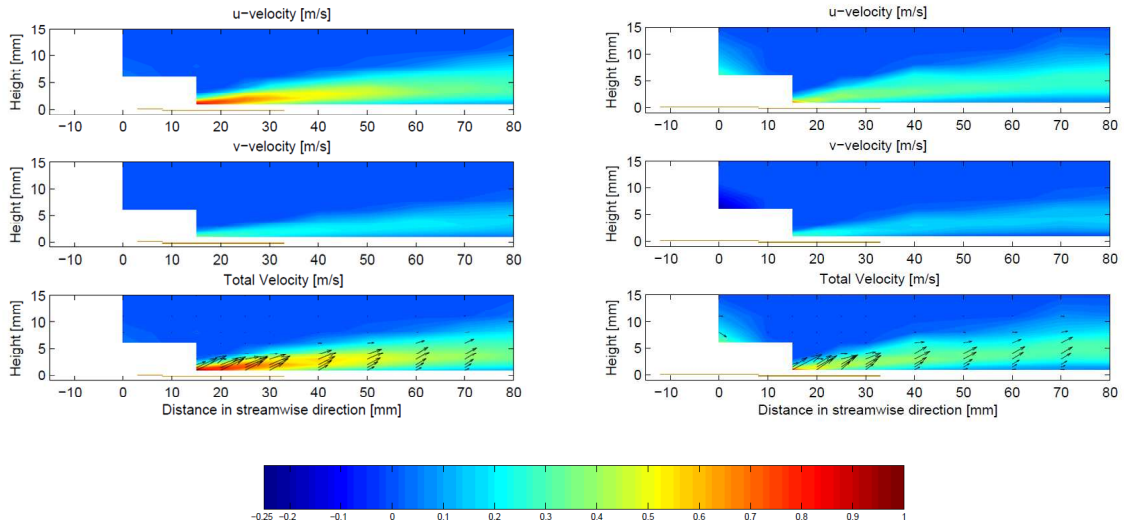


Figure 5. Typical flowfield for upper electrode length of (left) 5 mm (right) 20 mm

The induced flow under the variation of the length of the upper electrode (l_u) is shown in Figure 6. It is apparent that the induced velocity is slightly decreasing with increasing l_u . The sudden drop for $l_u = 15$ mm is attributed to a probable manufacturing error in the actuator. For the variation of the length of the lower electrode (l_l) it is apparent that a threshold length exists above which there is no significant influence in the induced flow (Figure 7). The plasma region is physically limited by the length of the grounded region below the dielectric. As soon as the length of the lower electrode exceeds the threshold, electron-ion recombination processes limit the plasma region independently of any further increase in l_l . Similar behavior is observed for the horizontal electrode gap (g) in Figure 8. It is apparent that for increasing gap the intensity of the electric field decreases with respective decrease in induced velocity. For negative gap (overlapping electrodes) no significant change in the flowfield is observed although considerable increase in travelling current has been registered. The dielectric thickness (Figure 9) is also directly related with the distance between the two electrodes which has a clear impact on the intensity of the electric field and the induced velocity. In general the induced flow appears to be more sensitive to variations of the distance of the inner edge of the electrodes (i.e. t_d and g).

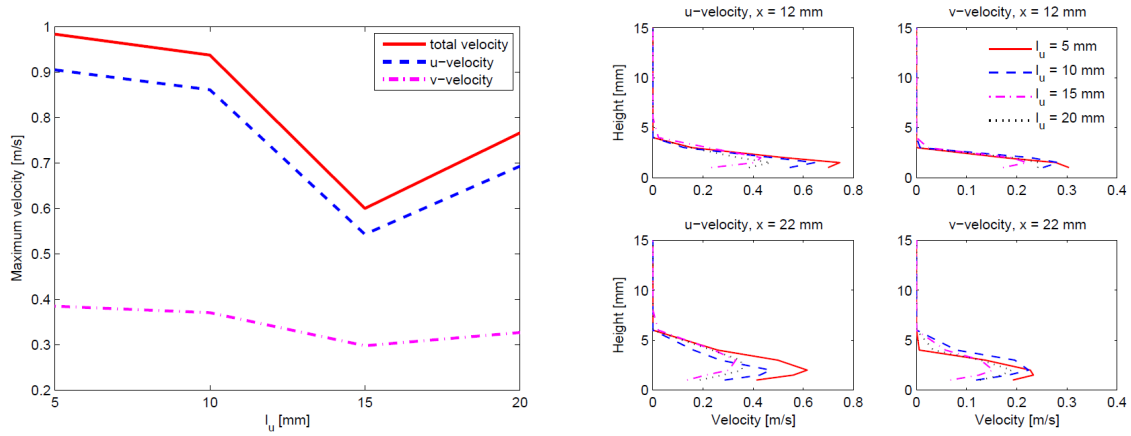


Figure 6. Maximum velocity and velocity profiles for I_u variation

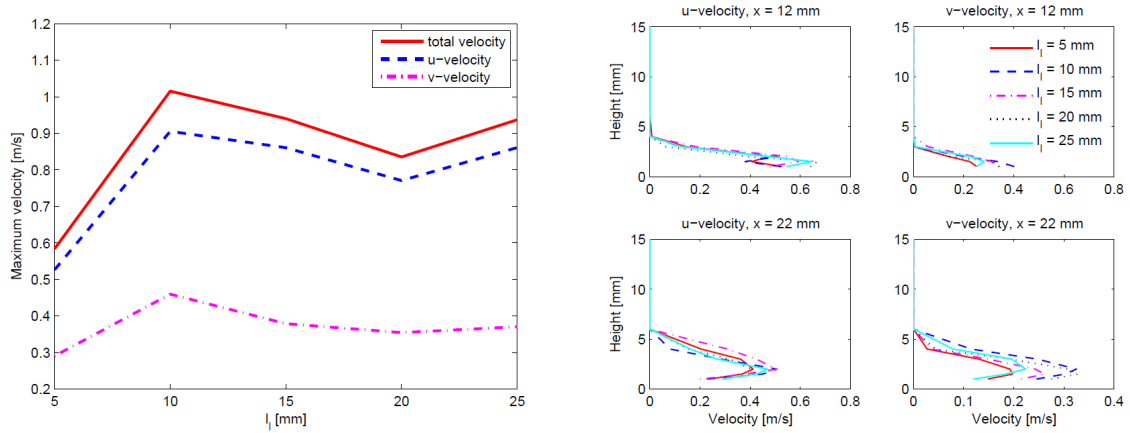


Figure 7. Maximum velocity and velocity profiles for I_l variation

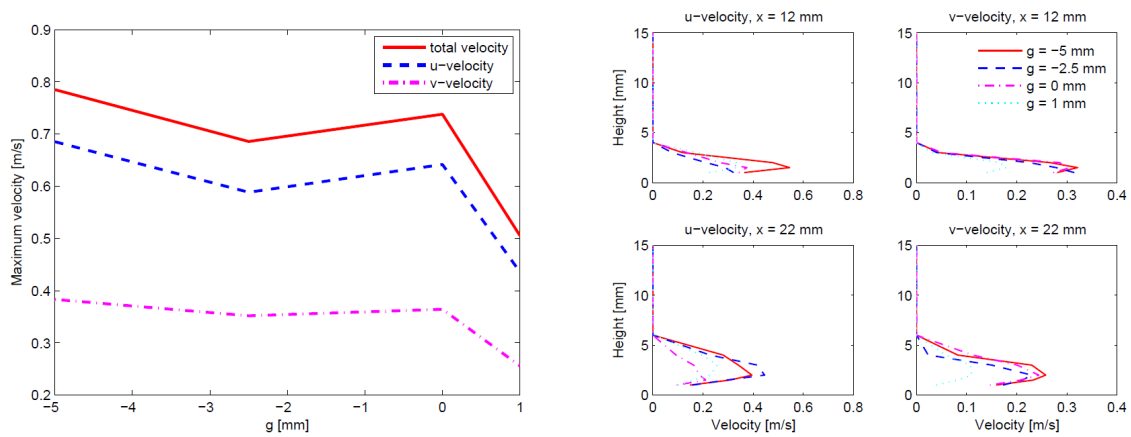


Figure 8. Maximum velocity and velocity profiles for g variation

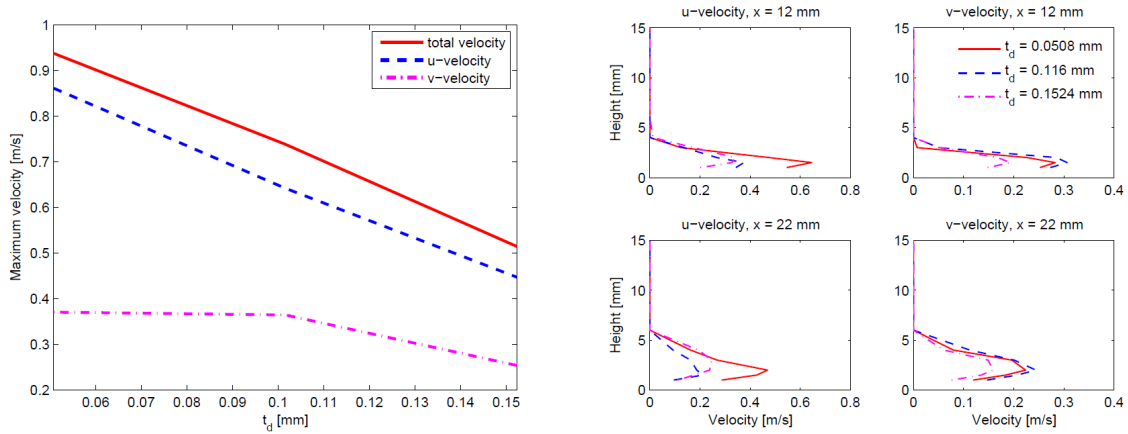


Figure 9. Maximum velocity and velocity profiles for t_d variation

Experiment group #2: electrical properties

The influence of the applied voltage (V_{app}) is presented in Figure 10. The induced velocity increases with V_{app} although it is reported by Forte et al. (2007) that a plateau is reached above 20 kV_{pp}. A larger voltage than 12 kV_{pp} is not investigated as maximizing the induced velocity was not in the scope of this research. The increase in frequency of applied voltage (F) has similar effects (Figure 11). Larger F is expected to provide further increase of induced velocity although the life of the dielectric barrier is severely reduced. Tested waveforms are presented in Figure 12 with the corresponding current from the amplifier's internal probe as well as the discharge current through the grounded electrode. For the variation in waveform of the applied voltage (Figure 13) it is clear that the increase in induced velocity is a function of the gradient of voltage. Square waveform appears to give the best results in terms of pure velocity. Nevertheless, the energy consumption is significantly larger than sine or triangle signals as the discharge current is more. For pulsed operation the induced velocity increases with increase of the duty cycle (D) (Figure 14). It is interesting to note that this behavior is not linear. For larger D the induced velocities are not as large as expected. One of the reasons for investigating the pulsed operation in more detail is to clarify this phenomenon. The pulsed frequency appears to have no influence.

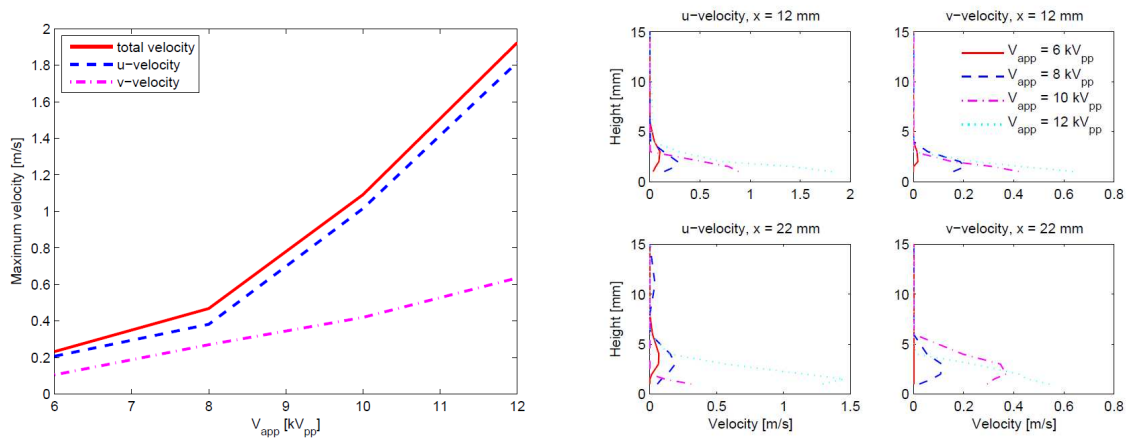


Figure 10. Maximum velocity and velocity profiles for V_{app} variation

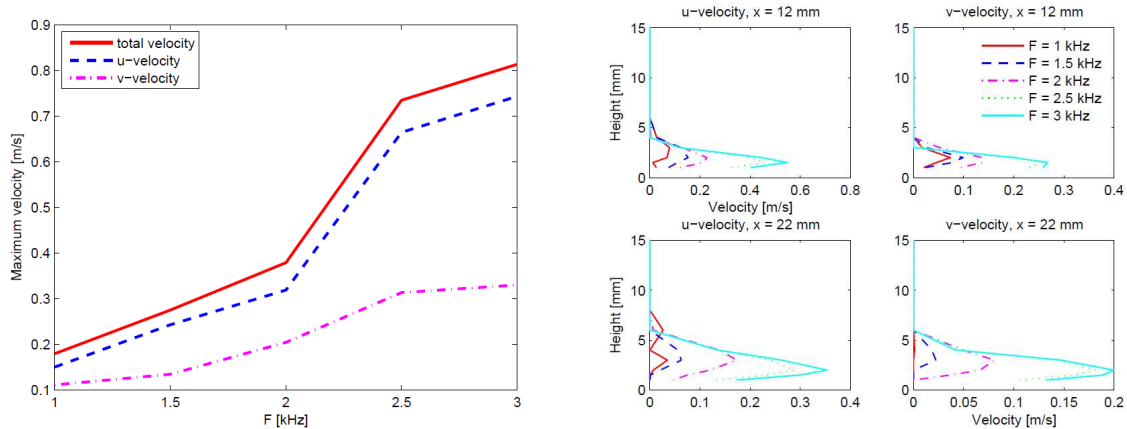


Figure 11. Maximum velocity and velocity profiles for F variation

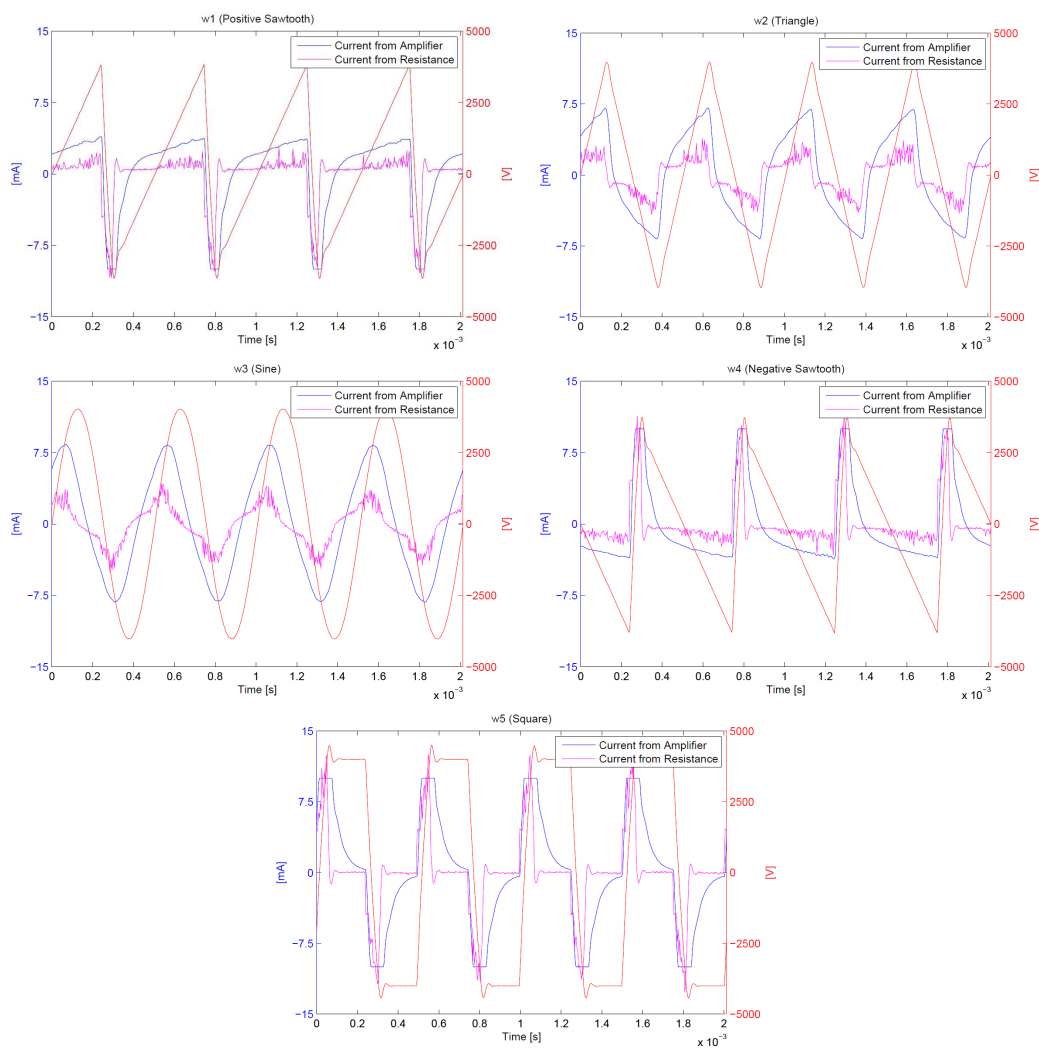


Figure 12. Tested waveforms and corresponding discharge current

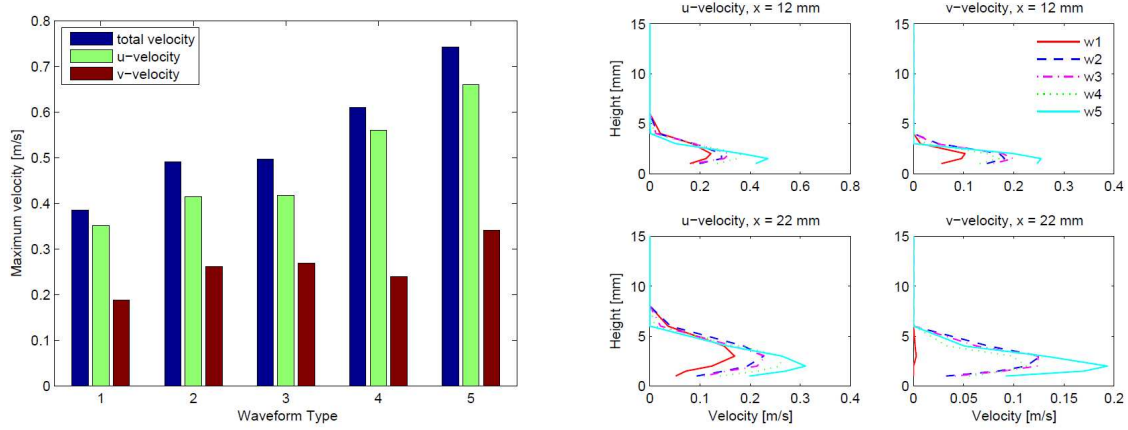


Figure 13. Maximum velocity and velocity profiles for waveform variation

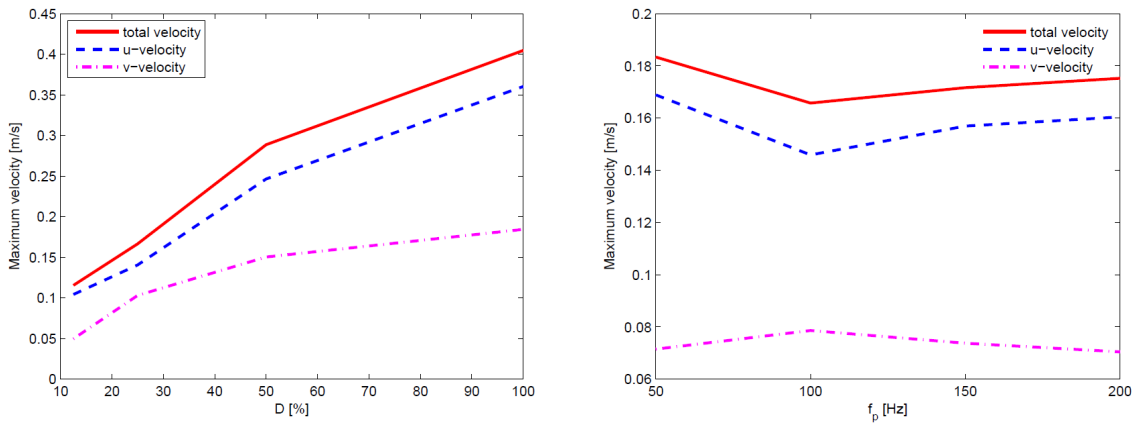


Figure 14. Maximum velocity for (left) D variation and (right) f_p variation

Experiment group #3: time resolved pulsed operation

The investigation for the time resolved operation is done at x-positions of 7 mm and 15 mm. A total of 14 points is measured in a direction perpendicular to the wall to accurately resolve the near-wall jet formation. At these positions data are taken at a sample rate of 100 kHz in order to sufficiently resolve the induced velocity fluctuations from the plasma operation. The response of the flow for different duty cycles is shown in Figure 15. For all cases except the 5% duty cycle the pulsed operation of the plasma is directly translated to a pulsed flowfield. Also evident is the extremely fast response of the flow which builds up to a quasi-steady state in only a few periods. Furthermore, an interesting phenomenon which is observed in mainly low D is the existence of two peaks at each velocity pulse. This could be attributed to the formation of a starting vortex. For the variation of the pulsed frequency (Figure 16) the pulsed behavior of the flow is retained although the amplitude of fluctuations becomes lower with higher f_p . The flow is less sensitive to faster fluctuations due to viscous and diffusive effects. In freestream conditions the fluctuations are expected to be larger since the induced flow and the boundary-layer flow are aligned. In general the flow responds well to the pulsed operation especially at low f_p and D an essential requirement for an efficient flow control actuator.

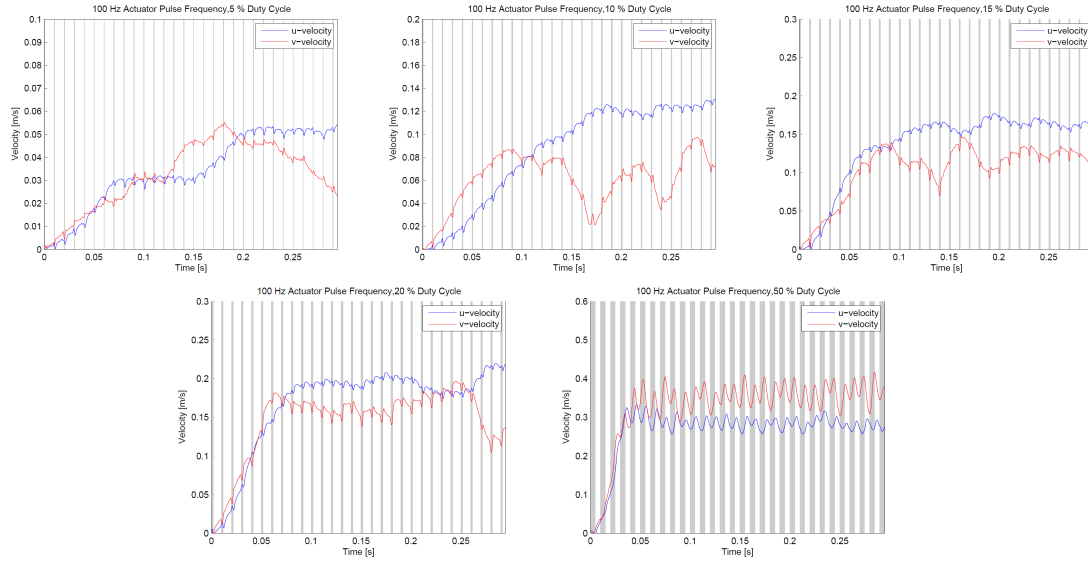


Figure 15. Flow response to variation of D ($x = 7$ mm, $y = 1.5$ mm) ⁴

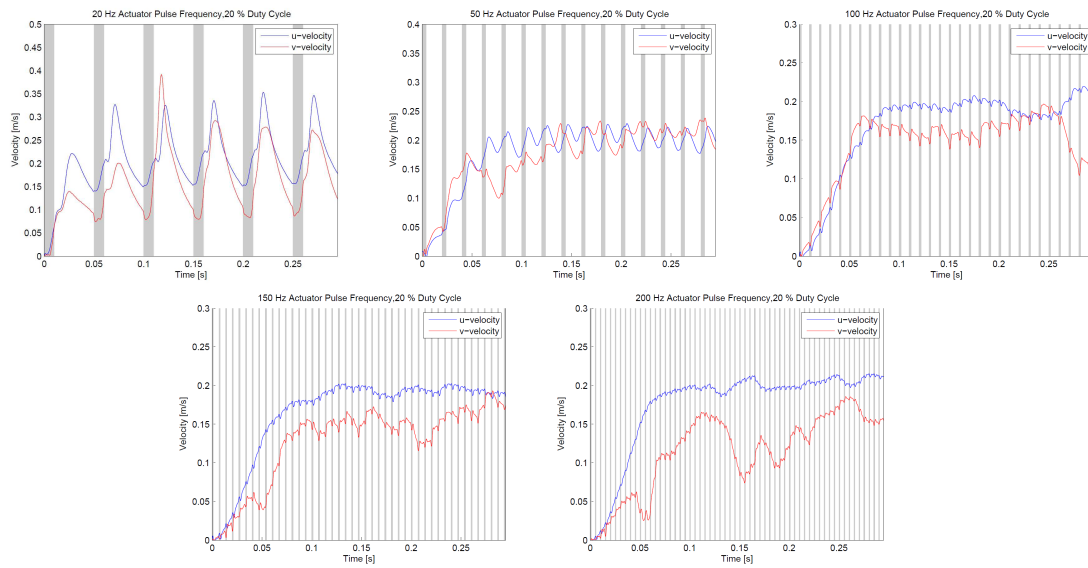


Figure 16. Flow response to variation of f_p ($x = 7$ mm, $y = 1.5$ mm)

CONCLUSION

The production of a small localized body force with an actuator that employs virtually no moving parts seems ideal for flow control applications especially in terms of robustness. This is especially important in the case of TS wave cancellation where the actuator has to be small, non-intrusive and responsive. The DBD actuator combines these characteristics with additional ease of manufacturing and energy efficiency. A parametric study has been conducted in order to investigate the influence of geometrical and electrical properties of the DBD actuator on the induced velocity flowfield. Additional

⁴ The grey shaded areas denote operation of the plasma actuator.

high sample-rate investigations on the pulsed operation indicate favorable properties for TS wave cancellation. Future experiments are planned to validate the concept of active cancellation of artificial and random TS waves using the DBD actuator.

ACKNOWLEDGMENTS

This study was done in the framework of Aerodynamic Drag Reduction within the CleanEra project (www.cleanera.tudelft.nl). The authors would like to thank dr.ir. Peter H.F. Morshuis from the High Voltage Laboratory of the Faculty of Electrical Engineering, Mathematics and Computer Science, for his valuable advice and help as well as ing. Stefan Bernardy and Leo Molenwijk for their technical assistance.

REFERENCES

- Schlichting, H. & Gersten, K. (2000), "Boundary Layer Theory", Springer.
- Thomas, A. S. W. (1983), "Control of boundary-layer transition using a wave-superposition principle." *Journal of Fluid Mechanics*, 137, 233-250
- Bower, W. W.; Kegelman, J. T.; Pal, A. & Meyer, G. H. (1987), "A numerical study of two-dimensional instability-wave control based on the Orr--Sommerfeld equation", *Physics of Fluids*, 30, 998-1004
- Sturzebecher, D. & Nitsche, W. (2003), "Active cancellation of Tollmien-Schlichting instabilities on a wing using multi-channel sensor actuator systems", *International Journal of Heat and Fluid Flow*, 2003, 24, 572-583
- Engert, M., Patzold, A. & Nitsche, W. (2007) "Development of a sensor-actuator-system for active control of boundary layer instabilities in compressible flows", *New Results in Numerical and Experimental Fluid Mechanics*, 96, 252-259
- Grundmann, S. & Tropea, C. (2008), "Active cancellation of artificially introduced Tollmien-Schlichting waves using plasma actuators", *Experiments in Fluids*, 44, 795-806
- R. Roth, Sherman, D. M. & Wilkinson, S. P. (2000), "Electrohydrodynamic flow control with a glow-discharge surface plasma", *AIAA journal*, 38, 1166-1172
- Post, M. L. & Corke, T. C. (2004), "Separation control on high angle of attack airfoil using plasma actuators", *AIAA Journal*, 42, 2177-2184
- Jacob, J. D.; Rivir, R.; Carter, C. & Estevadeordal, J. (2004), "Boundary layer flow control using AC discharge plasma actuators", 2nd AIAA Flow Control Conference
- Huang, J.; Corke, T. C. & Thomas, F. O. (2006), "Plasma Actuators for Separation Control of Low-Pressure Turbine Blades", *AIAA Journal*, 44, 51-57
- Jukes, T. N.; Choi, K. ..; Johnson, G. A. & Scott, S. J. (2006), "Turbulent drag reduction by surface plasma through spanwise flow oscillation", 3, 1687-1700
- Seraudie, A.; Aubert, E.; Naude, N. & Cambronne, (2006) J. P., "Effect of plasma actuators on a flat plate laminar boundary layer in subsonic conditions" 2, 1065-1073
- Forte, M.; Jolibois, J.; Pons, J.; Moreau, E.; Touchard, G. & Cazalens, M., (2007), "Optimization of a dielectric barrier discharge actuator by stationary and non-stationary measurements of the induced flow velocity: Application to airflow control", *Experiments in Fluids*, 43, 917-928
- Corke, T. C.; Post, M. L. & Orlov, D. M. (2007), "SDBD plasma enhanced aerodynamics: concepts, optimization and applications", *Progress in Aerospace Sciences*, 43, 193-217
- Jayaraman, B. & Shyy, W. (2008) "Modeling of dielectric barrier discharge-induced fluid dynamics and heat transfer" *Progress in Aerospace Sciences*, 44, 139-191